are the same as those for the gauche rotamer; the methylene protons appear as a singlet at $\delta = 4.09$). δ values are in ppm relative to Me_4Si.

Preparation of (6-Methyl-2-pyridyl)methyllithium. To a hexane solution of *n*-butyllithium was added 2,6-dimethylpyridine by syringe. The solution was stirred, butane was evolved, and a yellow precipitate formed. This was collected by filtration, dried in vacuo, and stored in sealed ampules.

X-ray Structural Determination. A crystal of dimensions 0.05 × 0.24 × 0.30 mm was mounted in a nitrogen-filled glovebag and transferred to the liquid-nitrogen boil-off cooling system of the diffractometer.[15] The diffractometer utilized for data collection was designed and constructed locally. A Picker four-circle goniostat equipped with a Furnas Monochromator (HOG crystal) and Picker X-ray generator was interfaced to a TI 980 minicomputer, with Slo-syn stepping motors to drive the angles. Centering was accomplished with use of top/bottom-left/right slit assemblies. The minicomputer is interfaced by low-speed data lines to a CYBER 172-CDC 6600 multimainframe system where all computations are performed.

The cell dimensions obtained from 36 reflections at −171 °C with Mo Kα (λ = 0.71069 Å) were $a = 22.013$ (5) Å, $b = 7.974$ (2) Å, $c = 14.933$ (3) Å, $\beta = 96.43$ (1)°, $V = 2604.74$ Å^3, $Z = 4$, $d_{calcd} = 1.480$ g. cm^{-3}, and space group $P2_1/a$.

A total number of 6282 reflections were collected by using standard moving-crystal moving-detector techniques with the following values: scan speed = 5° min^{-1}, scan width = 1.6 + dispersion, single background time at extremes of scan = 4 s, aperture size = 3.0 × 4.0 mm. The limits of the data collection were $5° < 2\theta < 50°$. The number of reflections with $F > 2.33\sigma(F)$ was 3383 of the 4621 unique amplitudes. The data were corrected for absorption (linear absorption coefficient = 9.591 cm^{-1}); minimum and maximum corrections were 0.7980 and 0.9080, respectively.

The structure was solved by a combination of direct and Fourier methods to give final residuals $RF = 0.0709$ and $R_wF = 0.0560$. The goodness of the fit for the last cycle was 1.416, and the maximum δ/σ for the last cycle was 0.09.

All of the hydrogen atoms, except for those on the two methyl groups of the pyridine ligands [C(19), C(27)] were located and refined with use of isotropic thermal parameters. All nonhydrogen atoms were refined anisotropically.

The final difference map contained several peaks ranging from 0.6 to 0.9 e/Å^3 in the vicinity of C(19), and C(27), possibly indicative of a disorder or rotation of those methyl groups.

(15) J. C. Huffman, Ph.D Thesis, Indiana University, Bloomington, Ind., 1974.

Acknowledgment. We thank the donors of the Petroleum Research Fund, administered by the American Chemical Society, the National Science Foundation, the Marshal H. Wrubel Computing Center, and the taxpayers of the State of Indiana for financial support of this work.

Registry No. $Mo_2(NMe_2)_4(CH_2pyMe)_2$, 76600-27-6; $Mo_2Cl_2(NMe_2)_4$, 63301-82-6; $LiCH_2pyMe$, 34667-18-0.

Supplementary Material Available: A table of anisotropic thermal parameters and a listing of observed and calculated structure factor amplitudes (32 pages). Ordering information is given on any current masthead page.

Contribution from Donnan Laboratories, University of Liverpool, Liverpool L69 3BX, U.K., the Department of Chemistry, University of Glasglow, Glasgow G12 8QQ, U.K., the Department of Chemistry, University of Western Ontario, London, Canada N6A 5B7, and the Inorganic Chemistry Laboratory, University of Oxford, Oxford OX1 3QR, U.K.

Synthesis, Structure, and Bonding in the Complex Cation $[Pt_2Me_3(\mu\text{-}Ph_2PCH_2PPh_2)_2]^+$: An Example of a Donor-Acceptor Metal-Metal Bond

MICHAEL P. BROWN,*[1a] SUSAN J. COOPER,[1a] AILEEN A. FREW,[1b] LJUBICA MANOJLOVIĆ-MUIR,*[1b] KENNETH W. MUIR,[1b] RICHARD J. PUDDEPHATT,*[1c] KENNETH R. SEDDON,[1d] and MARY A. THOMSON[1c]

Received August 5, 1980

Several preparative routes to the binuclear trimethyldiplatinum complex cation $[Pt_2Me_3(\mu\text{-}Ph_2PCH_2PPh_2)_2]^+$, isolated as the PF_6^-, SbF_6^-, or ClO_4^- salts, have been found, and some aspects of the mechanism of formation from mononuclear precursors have been elucidated. The complex as the PF_6^- salt crystallizes in the space group C_{2h}^5-$P2_1/n$ with four molecules in a unit cell whose dimensions are $a = 10.220$ (4) Å, $b = 25.522$ (6) Å, $c = 23.832$ (3) Å, and $\beta = 93.57$ (3)°. On the basis of 5467 independent reflections with $I \geq 3\sigma(I)$, the structure was refined by full-matrix least-squares techniques to conventional agreement indices of $R = 0.081$ and $R_w = 0.13$. The complex cation contains a Pt–Pt separation of 2.769 Å formulated as a $Pt^{II} \rightarrow Pt^{II}$ donor-acceptor bond. This formulation is supported by consideration of the NMR coupling constants derived from analysis of the complex ^1H and ^{31}P NMR spectra. The Pt–Pt bond in this complex has a lower trans influence than Pt–Pt homopolar bonds in binuclear platinum(I) complexes.

Introduction

All known complexes of formula $[Pt_2X_2(Y)(dppm)_2]^{n+}$ ($n = 0$, 1; dppm = $Ph_2PCH_2PPh_2$), e.g., I–V, have "A-frame" structures, and the hydride $[Pt_2H_3(dppm)_2]^+$ (VI) is no exception even though the $Pt_2(\mu\text{-H})$ grouping is electron deficient.[2,3] The existence of this trihydridodiplatinum complex cation prompted us to consider whether the trimethyldiplatinum complex cation $[Pt_2Me_3(dppm)_2]^+$ might exist and, if so, what type of structure it might have. On the one hand, it seemed unlikely that it would adopt an A-frame structure because that implied formation of an electron-deficient Pt_2-

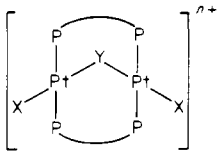

$n = 0$, X = Cl
I, Y = SO_2
II, Y = CH_2
III, Y = CO

$n = 1$, X = CH_3
IV, Y = Cl

$n = 1$, X = H
V, Y = SMe
VI, Y = H

(1) (a) University of Liverpool. (b) University of Glasgow. (c) University of Western Ontario. (d) University of Oxford.
(2) Brown, M. P.; Puddephatt, R. J.; Rashidi, M.; Seddon, K. R. *J. Chem. Soc., Dalton Trans.* **1978**, 516.
(3) (a) Brown, M. P.; Keith, A. N.; Manojilović-Muir, Lj.; Muir, K. W.; Puddephatt, R. J.; Seddon, K. R. *Inorg. Chim. Acta* **1979**, *34*, L223. (b) Brown, M. P.; Fisher, J. R.; Puddephatt, R. J.; Seddon, K. R. *Inorg. Chem.* **1979**, *18*, 2808.

0020-1669/81/1320-1500$01.25/0

(μ-CH_3) bridge; on the other hand, it was difficult to envisage an alternative structure. We therefore decided to attempt the synthesis of this complex, and our results are reported herein. In fact, we were able to obtain $[Pt_2Me_3(dppm)_2]^+$ readily and several preparative routes are described. We show that it does not adopt the A-frame structure but has instead an unusual type of binuclear geometry, previously exhibited by only one other transition metal complex, namely, $[Rh(CO)RhCl_2\{\mu\text{-}(PhO)_2PN(Et)P(OPh)_2\}_2]$.[4] An interesting feature of its structure is, however, the Pt–Pt distance of 2.769 Å which is, we propose, explained by the formation of a Pt–Pt donor–acceptor bond. Preliminary accounts of this work have been published elsewhere.[5,6]

Experimental Section

The synthesis of methylplatinum precursors has been described elsewhere.[7,8] NMR spectra were recorded on a Varian XL100 or a Bruker WH-200 spectrometer. The reference for ^{31}P NMR spectra was trimethyl phosphate in acetone-d_6, and the sign convention of negative upfield shifts and positive downfield shifts has been adopted as described previously.[3]

Preparations of $[Pt_2Me_3(\mu\text{-dppm})_2]X$ {X = $[PF_6]$, $[SbF_6]$, or $[ClO_4]$}. (i) From $[PtMe_2(dppm)]$ and $[PtCl_2(dppm)]$. A mixture of $[PtMe_2(dppm)]$ (1.86 g, 3.1 mmol) and $[PtCl_2(dppm)]$ (0.66 g, 1.02 mmol) in methanol (60 mL) was refluxed for 1 h. Filtration of the deep yellow solution thus formed yielded a small amount of unreacted $[PtCl_2(dppm)]$ (0.20 g, 0.31 mmol) as a white solid. Potassium hexafluorophosphate (1.2 g, 6.5 mmol) was added, the solution was reheated to boiling for 15 min, and then some of the solvent was evaporated in a stream of dinitrogen. The solution (~40 mL) was cooled and water added very slowly to precipitate the yellow product, which was filtered off and partially dried. It was then dissolved in dichloromethane, dried further, and recrystallized by slow addition of hexane to yield pure $[Pt_2Me_3(\mu\text{-dppm})_2][PF_6]$ as a yellow crystalline solid (1.40 g, 68% based on Pt content of $[PtMe_2(dppm)]$). Anal. Calcd for $[Pt_2Me_3(\mu\text{-dppm})_2][PF_6]$: C, 47.2; H, 4.0; F, 8.5; P, 11.5. Found: C, 47.0; H, 3.8; F, 8.6; P, 11.3. Attempts to obtain more product from the mother liquor yielded only a dark red oil, and hence the solvent was evaporated completely to leave an unidentified red-brown residue (0.88 g). In a number of similar experiments the yields of pure product varied between 50 and 69%.

The hexafluoroantimonate $[Pt_2Me_3(\mu\text{-dppm})_2][SbF_6]$ was readily obtained in similar yields by the same method but by using $KSbF_6$ in place of KPF_6. It was characterized by its identical ^1H NMR spectrum and the presence of peaks in the infrared spectrum due to SbF_6^- (291 and 659 cm^{-1}).

(ii) From $[PtMe_2(dppm)]$ and $[PtCl(Me)(dppm)]$ in Methanol. A mixture of $[PtMe_2(dppm)]$ (0.0700 g, 0.11 mmol) and $[PtCl(Me)(dppm)]$ (0.0724 g, 0.11 mmol) was refluxed in methanol (3 mL) for 1 h. The deep orange solution thus formed was cooled and filtered to remove a trace (~0.01 g) of insoluble white material. The solvent was removed in a stream of dinitrogen and the residue dried in vacuo. ^1H NMR (220 MHz) examination of this residue in dichloromethane-d_2 showed the presence only of the $[Pt_2Me_3(\mu\text{-dppm})_2]^+$ cation present as essentially pure $[Pt_2Me_3(\mu\text{-dppm})_2]Cl$. Treatment with potassium hexafluorophosphate gave crystals of $[Pt_2Me_3(\mu\text{-dppm})_2][PF_6]$ (0.104 g, 67%) when the solution was worked up as in (i).

This experiment was repeated by using the dimer $[Pt_2Me_2(\mu\text{-Cl})(\mu\text{-dppm})_2]Cl$ in place of $[PtCl(Me)(dppm)]$. The color of the solution became deep yellow, but the reactants only partially dissolved. The solvent was replaced as above except that filtration was omitted. The ^1H NMR spectrum revealed the presence of only the starting materials. No peaks due to $[Pt_2Me_3(\mu\text{-dppm})_2]^+$ were observed. The limit of detection was probably 5–10% reaction.

(iii) From $[PtMe_2(dppm)]$ and $[PtCl(Me)(dppm)]$ in Dichloromethane/Methanol. A mixture of $[PtMe_2(dppm)]$ (0.0700 g, 0.11 mmol) and $[PtCl(Me)(dppm)]$ (0.0724 g, 0.11 mmol) was dissolved in dichloromethane (2 mL), and methanol (2 mL) was then added, producing an immediate yellow coloration. The solution was allowed to stand for ~60 h by which time the color had deepened to yellow-orange. The solvent was replaced with dichloromethane-d_2 as described in (ii). The ^1H NMR spectrum showed the presence of only $[Pt_2Me_3(\mu\text{-dppm})_2]^+$.

This experiment was also repeated by using $[Pt_2Me_2(\mu\text{-Cl})(\mu\text{-dppm})_2]$ in place of $[PtCl(Me)(dppm)]$, but no reaction occurred, even after ~30 days.

(iv) From $[PtMe_2(dppm)]$ and Hexafluorophosphoric Acid. Since solutions of HPF_6 are inevitably impure due to hydrolysis of PF_6^- ion and contain much more H^+ than indicated by the nominal concentration, it was necessary to determine the optimum quantity for reaction by trial and error. The relative quantities employed below appear to give the best results.

Aqueous HPF_6 (0.0430 g, 0.0260 mL of 65% w/v solution, nominally 0.12 mmol) and some dichloromethane (3 mL) were placed in a flask (250 mL) fitted with a serum cap. The solvent and the vapor above it were allowed to equilibrate, and the excess pressure was released through a needle. The flask was then placed in an ice bath, and a solution of $[PtMe_2(dppm)]$ (0.359 g, 0.589 mmol) in dichloromethane (5 mL) at 0 °C was added with stirring. A yellow color was immediately produced. Stirring was continued for 10 min. Analysis of the gas phase by GLC revealed the formation of methane (0.271 mmol, 92%). The chromatograph was calibrated with standard mixtures produced in an identical 250-mL flask containing the same volume of solvent. The solution remaining in the flask was worked up in the usual way, after addition of more PF_6^- ion in the form of the potassium salt, to afford crystalline $[Pt_2Me_3(\mu\text{-dppm})_2][PF_6]$ (0.268 g, 67%) identified by its IR spectrum.

(v) From $[PtMe_2(dppm)]$ and Hexafluoroantimonic Acid. A mixture of $[PtMe_2(dppm)]$ (0.176 g, 0.288 mmol), $HSbF_6 \cdot 6H_2O$ (0.0341 g, 0.098 mmol) and dichloromethane (3 mL) was allowed to react under the same conditions as in iv. After addition of more SbF_6^- ion in the form of a $KSbF_6$ (0.025 g) suspension in methanol, the reaction mixture was worked up in the usual way to afford crystals of $[Pt_2Me_3(\mu\text{-dppm})_2][SbF_6]$ (0.148 g, 72%).

(vi) From $[PtMe_2(dppm)]$ and Perchloric Acid. The aqueous acid (72%) was diluted approximately 100-fold with acetone, and the solution was standardized. An aliquot (~3 mL, containing 0.41 mmol of perchloric acid) was added slowly with stirring to an acetone solution of $[PtMe_2(dppm)]$ (0.50 g, 0.82 mmol in 20 mL) contained in a flask fitted with a rubber septum. After a further 10 min of stirring, analysis of the gas above the solution by GLC showed that methane (0.38 mmol) was present. Attempts to isolate a crystalline product were not very successful although a mainly amorphous solid (0.26 g) was obtained. Its infrared spectrum was poorly resolved but showed the presence of ClO_4^- (627 and 1092 cm^{-1}) and, making allowance for the change of anion, was similar to that of $[Pt_2Me_3(\mu\text{-dppm})_2][PF_6]$. Its ^1H NMR spectrum in CD_2Cl_2 (220 MHz) revealed $[Pt_2Me_3(\mu\text{-dppm})_2]^+$ as the only detectable species.

X-ray Structure Analysis of $[Pt_2Me_3(\mu\text{-dppm})_2][PF_6]\cdot 3CH_2Cl_2$. (a) Data Collection and Reduction. Crystals suitable for diffraction measurements were obtained by slow cooling of a saturated solution of $[Pt_2Me_3(\mu\text{-dppm})_2][PF_6]$ in CH_2Cl_2/hexane. They were yellow prisms, which were extremely sensitive to light and which cracked rapidly when removed from the mother liquor. Several specimens were sealed in Lindemann glass capillaries so that each was in contact with a drop of mother liquor.

All X-ray measurements were made with an Enraf-Nonius CAD-4F diffractometer. Preliminary investigation of several crystals established that the Laue group is $2/m$ and the crystal lattice is primitive. The observed systematic absences, $h0l$ for $h + l \neq 2n$ and $0k0$ for $k \neq 2n$, were consistent with the space group C_{2h}^5-$P2_1/n$ (an alternative setting of $P2_1/c$, No. 14). The crystal used for the final measurements was a prism of approximate dimensions 0.23 × 0.23 × 0.43 mm. After optical examination and centering on the diffractometer, the crystal was protected from light by coating the capillary with an opaque paint and by maintaining darkness in the laboratory.

The unit cell dimensions, shown in Table I, were obtained by a least-squares treatment of the setting angles of 25 automatically centered reflections with $12 \leq \theta(\text{Mo } K\alpha) \leq 17°$. The intensities of 8287 hkl and $hk\bar{l}$ reflections with $3 \leq \theta(\text{Mo } K\alpha) \leq 22°$ were measured

(4) Haines, R. J.; Meintjies, E.; Laing, M. *Inorg. Chim. Acta* **1979**, *36*, L403.
(5) Brown, M. P.; Cooper, S. J.; Puddephatt, R. J.; Thomson, M. A.; Seddon, K. R. *J. Chem. Soc., Chem. Commun.* **1979**, 1117.
(6) Frew, A. A.; Manojlović-Muir, Lj.; Muir, K. W. *J. Chem. Soc., Chem. Commun.*, in press.
(7) Cooper, S. J.; Brown, M. P.; Puddephatt, R. J., submitted for publication in *Inorg. Chem.*
(8) Appleton, T. G.; Bennett, M. A.; Tomkins, I. B. *J. Chem. Soc., Dalton Trans.* **1976**, 439.

Table I. Crystal Data for $[Pt_2Me_3(\mu\text{-dppm})_2][PF_6]\cdot 3CH_2Cl_2$

a, Å	10.220 (4)[a]	empirical formula	$C_{56}H_{59}Cl_6F_6P_5Pt_2$
b, Å	25.522 (6)	fw	1603.84
c, Å	23.832 (3)	space group	C_{2h}^5-$P2_1/n$
β, deg	93.57 (3)	temp, °C	20 ± 1
V, Å^3	6204	radiation	Mo Kα (λ 0.710 69 Å)
Z	4	monochromator	mosaic graphite crystal
d, g cm^{-3}	1.72 (calcd)	μ(Mo Kα), cm^{-1}	49.9

[a] Throughout this paper standard deviations are given in parentheses after the quantity to which they refer in units of the least significant digit.

using the $\theta/2\theta$ scan technique. For each reflection the scan range, centered on the $K\alpha$ position, was 0.97° in θ. The counts accumulated in the first and last quarters of the scan range (B_1 and B_2) were taken to represent the local background. The integrated intensity, I, and its standard deviation $\sigma_1(I)$, were determined from the relationships $I = C - 2(B_1 + B_2)$ and $\sigma_1(I) = [C + 4(B_1 + B_2)]^{1/2}$, where C is the count accumulated in the second and third quarters of the scan range. Reflections for which a preliminary scan, taken at a speed of 7°/min, gave $\sigma_1(I)/I > {}^1/_2$ were considered weak and not examined further. Each of the other reflections was scanned with the speed adjusted to achieve a final $\sigma_1(I)/I$ ratio of 0.03, subject to a maximum counting time of 90 s; the scan was the repeated, and the two results were checked for consistency. For 87 reflections consistent results were not obtained even after two repetitions. A check on these reflections at the end of structure analysis revealed none for which disagreement between $|F_o|$ and $|F_c|$ would warrant rejection from the calculations. The crystal orientation, periodically checked throughout the experiment, showed no change in a setting angle larger than 0.1°. The intensities of two reflections remeasured every 2 h fluctuated randomly by ±5% and ±2% from their mean values.

The integrated intensities and their standard deviations $\sigma(I)$, where $\sigma^2(I) = \sigma_1^2(I) + (qI)^2$ and $q = 0.04$, were corrected for Lorentz and polarization effects. Correction for absorption was precluded by obstacles to required measurements of the crystal specimen. However, the shape of the crystal used in this analysis diminishes the importance of such a correction. Rejection of 2474 reflections, for which $I \leq 3\sigma(I)$, and merging of 173 $0kl$, $0k\bar{l}$ pairs (R for merging = 0.039 on F) yielded 5467 independent structure amplitudes which were used in further calculations.

(b) Structure Solution and Refinement. The positions of the platinum atoms were deduced from a three-dimensional Patterson function and those of the remaining non-hydrogen atoms from subsequent difference syntheses. The scale factor and the positional and thermal atomic parameters were refined by full-matrix least-squares minimization of the function $\sum w(|F_o| - |F_c|)^2$, where $w = 1/\sigma^2(|F_o|)$. The phenyl rings were treated as rigid bodies, constrained to $6/mmm$ symmetry with C–C bond lengths of 1.395 Å. The nonhydrogen atoms of the $[Pt_2Me_3(dppm)_2]^+$ and PF_6^- ions were assigned anisotropic thermal parameters, except for the phenyl carbon atoms for which isotropic thermal vibrations were assumed. The refinement of this model converged at $R = 0.12$ and $R_w = 0.18$ ($R = \sum(||F_o| - |F_c||)/\sum|F_o|$ and $R_w = [\sum w(|F_o| - |F_c|)^2/\sum wF_o^2]^{1/2}$).

A subsequent difference synthesis displayed prominent peaks upon which the nonhydrogen atoms of three distorted dichloromethane molecules could be superimposed. Hence, nine chlorine and carbon atoms of the solvent molecules were included in the refinement with isotropic thermal parameters, and this led to the final values of R and R_w of 0.081 and 0.13. The atomic scattering factors and the anomalous dispersion corrections for platinum, chlorine, and phosphorus atoms were taken from ref 9. Scattering of the hydrogen atoms was not accounted for.

In the final difference synthesis the function values range from −1.2 to +1.4 e Å^{-3}, the highest peaks being associated with the positions of chlorine and platinum atoms. An analysis of $\sum w(|F_o| - |F_c|)^2$ as a function of $|F_o|$, $\sin\theta$, and Miller indices revealed no obvious trends. However, the list of the final $|F_o|$ and $|F_c|$ values[10] shows rather large discrepancies for a number of reflections that are dispersed through reciprocal space. We feel that these discrepancies arise predominantly from deficiencies of the refined structural models for the PF_6^- ion

(9) "International Tables for X-ray Crystallography"; Kynoch Press: Birmingham, England, 1974; Vol. IV, Tables 2.2B and 2.3.1.
(10) Supplementary material.

Table II. Final Coordinates and Isotropic Thermal Parameters

atom	x	y	z	U, Å^2
Pt(1)	30593 (10)	2288 (4)	27584 (4)	
Pt(2)	10961 (10)	−716 (4)	34409 (4)	
P(1)	1210 (7)	691 (3)	3927 (3)	
P(2)	2400 (7)	1090 (3)	2852 (3)	
P(3)	883 (7)	−863 (3)	2990 (3)	
P(4)	1734 (7)	−152 (3)	2034 (3)	
P(5)	3832 (13)	2647 (4)	4785 (4)	
F(1)	3971 (24)	2969 (14)	4245 (12)	
F(2)	3562 (32)	2343 (12)	5317 (11)	
F(3)	4495 (54)	2131 (13)	4522 (14)	
F(4)	2540 (36)	2369 (14)	4448 (12)	
F(5)	5247 (34)	2826 (15)	5061 (11)	
F(6)	3092 (67)	3109 (14)	4961 (18)	
C(1)	1981 (32)	1232 (9)	3567 (11)	
C(2)	1164 (29)	−821 (10)	2230 (11)	
C(3)	4415 (30)	429 (10)	3411 (10)	
C(4)	4098 (29)	−478 (11)	2721 (12)	
C(5)	−292 (39)	−315 (14)	3972 (12)	
C(6)	−389 (18)	972 (8)	4063 (9)	48 (7)
C(7)	−1302 (18)	1010 (8)	3604 (9)	104 (14)
C(8)	−2531 (18)	1230 (8)	3673 (9)	140 (19)
C(9)	−2847 (18)	1412 (8)	4200 (9)	77 (9)
C(10)	−1934 (18)	1373 (8)	4658 (9)	63 (8)
C(11)	−705 (18)	1153 (8)	4589 (9)	93 (13)
C(12)	2123 (17)	643 (6)	4606 (6)	39 (6)
C(13)	2544 (17)	1097 (6)	4890 (6)	71 (9)
C(14)	3327 (17)	1059 (6)	5389 (6)	65 (8)
C(15)	3690 (17)	569 (6)	5604 (6)	76 (10)
C(16)	3270 (17)	115 (6)	5321 (6)	64 (9)
C(17)	2486 (17)	152 (6)	4821 (6)	42 (6)
C(18)	3736 (17)	1554 (7)	2767 (8)	57 (8)
C(19)	4597 (17)	1439 (7)	2353 (8)	48 (7)
C(20)	5611 (17)	1785 (7)	2250 (8)	84 (11)
C(21)	5763 (17)	2246 (7)	2562 (8)	68 (8)
C(22)	4901 (17)	2361 (7)	2976 (8)	69 (9)
C(23)	3888 (17)	2015 (7)	3079 (8)	60 (8)
C(24)	1116 (17)	1382 (7)	2377 (7)	39 (6)
C(25)	144 (17)	1711 (7)	2565 (7)	59 (8)
C(26)	−755 (17)	1946 (7)	2178 (7)	73 (9)
C(27)	−683 (17)	1851 (7)	1604 (7)	108 (13)
C(28)	289 (17)	1522 (7)	1417 (7)	64 (8)
C(29)	1188 (17)	1288 (7)	1804 (7)	72 (10)
C(30)	1984 (18)	−1364 (6)	3281 (7)	60 (9)
C(31)	2669 (18)	−1265 (6)	3794 (7)	56 (7)
C(32)	3484 (18)	−1648 (6)	4044 (7)	65 (9)
C(33)	3614 (18)	−2132 (6)	3780 (7)	86 (11)
C(34)	2928 (18)	−2232 (6)	3267 (7)	39 (6)
C(35)	2113 (18)	−1848 (6)	3017 (7)	55 (8)
C(36)	−721 (15)	−1174 (7)	2988 (8)	38 (6)
C(37)	−1674 (15)	−1004 (7)	2585 (8)	98 (12)
C(38)	−2942 (15)	−1208 (7)	2579 (8)	79 (10)
C(39)	−3255 (15)	−1582 (7)	2976 (8)	112 (13)
C(40)	−2301 (15)	−1752 (7)	3379 (8)	74 (10)
C(41)	−1034 (15)	−1548 (7)	3386 (8)	54 (7)
C(42)	2589 (20)	−275 (8)	1423 (7)	46 (7)
C(43)	3711 (20)	17 (8)	1333 (7)	102 (14)
C(44)	4425 (20)	−85 (8)	865 (7)	90 (12)
C(45)	4018 (20)	−478 (8)	487 (7)	85 (11)
C(46)	2897 (20)	−770 (8)	577 (7)	80 (10)
C(47)	2182 (20)	−669 (8)	1045 (7)	62 (9)
C(48)	167 (17)	130 (8)	1776 (9)	48 (7)
C(49)	−677 (17)	274 (8)	2188 (9)	66 (9)
C(50)	−1910 (17)	480 (8)	2031 (9)	101 (12)
C(51)	−2300 (17)	542 (8)	1464 (9)	91 (12)
C(52)	−1456 (17)	397 (8)	1052 (9)	112 (15)
C(53)	−223 (17)	191 (8)	1209 (9)	84 (11)
C(54)	214 (44)	3155 (17)	3772 (17)	104 (13)
C(55)	1741 (100)	1141 (41)	9670 (40)	282 (43)
C(56)	414 (89)	2764 (34)	5705 (34)	221 (34)
Cl(1)	1027 (13)	3088 (5)	3139 (5)	117 (4)
Cl(2)	−854 (18)	2587 (7)	3770 (7)	165 (6)
Cl(3)	2000 (22)	1127 (8)	8907 (9)	202 (8)
Cl(4)	1641 (29)	718 (12)	9952 (12)	266 (12)
Cl(5)	−708 (35)	2568 (14)	5396 (13)	339 (17)
Cl(6)	−327 (27)	3596 (11)	5780 (11)	257 (11)

[a] Fractional coordinates have been multiplied by 10^n ($n = 5$ for Pt and 4 for all other atoms). [b] The form of the isotropic temperature factor is $\exp[-8 \times 10^{-3}\pi^2 U((\sin\theta)/\lambda)^2]$.

Table III. Anisotropic Thermal Parameters[a]

atom	U_{11}	U_{22}	U_{33}	U_{23}	U_{13}	U_{12}
Pt(1)	336 (6)	380 (6)	355 (6)	21 (4)	40 (4)	9 (4)
Pt(2)	401 (7)	334 (6)	419 (7)	−6 (4)	105 (5)	−19 (5)
P(1)	44 (4)	38 (4)	43 (4)	6 (3)	12 (3)	−3 (3)
P(2)	41 (4)	38 (4)	37 (4)	6 (3)	6 (3)	2 (3)
P(3)	35 (4)	37 (4)	48 (4)	−1 (3)	5 (3)	−2 (3)
P(4)	49 (4)	38 (4)	40 (4)	1 (3)	1 (3)	4 (3)
P(5)	123 (10)	67 (6)	68 (7)	1 (5)	−26 (7)	11 (6)
F(1)	101 (18)	227 (36)	169 (24)	−5 (23)	−16 (17)	−66 (21)
F(2)	174 (28)	152 (25)	120 (20)	28 (18)	42 (20)	59 (23)
F(3)	434 (73)	136 (25)	131 (29)	18 (22)	60 (39)	153 (37)
F(4)	217 (34)	207 (35)	132 (22)	4 (22)	−113 (23)	37 (28)
F(5)	217 (34)	235 (39)	81 (18)	66 (22)	−27 (21)	−70 (31)
F(6)	460 (100)	129 (27)	260 (41)	45 (28)	219 (57)	139 (45)
C(1)	122 (25)	17 (13)	51 (16)	−10 (11)	40 (17)	−22 (15)
C(2)	61 (19)	36 (15)	44 (17)	12 (12)	11 (15)	−9 (13)
C(3)	98 (22)	32 (15)	29 (14)	−15 (11)	0 (14)	5 (15)
C(4)	58 (19)	48 (17)	56 (18)	−6 (14)	2 (15)	−17 (15)
C(5)	105 (31)	93 (25)	37 (17)	−3 (17)	44 (19)	−56 (24)

[a] The form of the anisotropic temperature factor is $\exp[-2\pi^2 \times 10^n \Sigma_{i=1}{}^3\Sigma_{j=1}{}^3 U_{ij}h_ih_ja^*_ia^*_j]$, with $n = 4$ for Pt and 3 for other atoms.

and CH_2Cl_2 molecules (see below).[6]

The final values of the positional and thermal atomic parameters are presented in Tables II and III. The computer programs used in this work are listed in ref 11.

Results and Discussion

Synthesis of the Complexes. The novel complex cation $[Pt_2Me_3(\mu\text{-dppm})_2]^+$ (VII), in the form of its PF_6^- (VIIa), SbF_6^- (VIIb), and ClO_4^- (VIIc) salts, may be readily synthesized by several methods. Our original intention was to attempt the synthesis of VII from the chloromethyl complex [PtCl(Me)(dppm)] (VIII) in the form of its dimer $[Pt_2Me_2(\mu\text{-Cl})(\mu\text{-dppm})_2]Cl$ (IX).[7] As a possible alternative preparation of VIII and IX we were therefore studying the reaction between $[PtMe_2(dppm)]$ and $[PtCl_2(dppm)]$ in boiling methanol and had the good fortune to obtain VII directly, in good yield. In fact, we have been unable to isolate VIII and IX as products of this reaction. However, it seemed likely that one or the other of these two chloromethyl complexes would be formed as an intermediate in this synthesis of the trimethyldiplatinum complex (VII), and so we put this to the test by using samples of these complexes obtained by other methods. Thus, under the same conditions as the above reaction, namely, under reflux in methanol, we found that the monomer VIII reacts readily with $[PtMe_2(dppm)]$ affording VII in high yield. In contrast, the dimer IX does not appear to react at all under these conditions. It therefore seems probable that the reaction between $[PtMe_2(dppm)]$ and $[PtCl_2(dppm)]$ proceeds as in (1) and (2).

$$[PtMe_2(dppm)] + [PtCl_2(dppm)] \rightarrow 2\underset{\text{VIII}}{[PtCl(Me)(dppm)]} \quad (1)$$

$$[PtMe_2(dppm)] + \underset{\text{VIII}}{[PtCl(Me)(dppm)]} \rightarrow \underset{\text{VII}}{[Pt_2Me_3(\mu\text{-dppm})_2]^+} + Cl^- \quad (2)$$

Moreover, the fact that the dimer IX could not be isolated from the reaction products (although it is possible that a very small amount is formed) indicates that reaction 2, observed separately in reactions starting directly from VIII, proceeds more rapidly than the dimerization reaction of VIII. This is surprising, since when VIII is refluxed in methanol, IX is readily obtained.[7] The reaction described by eq 2 was also observed to occur, although more slowly, at room temperature in solution in a mixture of dichloromethane and methanol, again conditions which normally favor dimerization of VIII.

Reaction of $[PtMe_2(dppm)]$ with acids HX (X = PF_6, SbF_6, and ClO_4) also provides a convenient route to the trimethyldiplatinum complex VII. Although all three acids give high yields of the cation in solution, isolation of a crystalline complex is best achieved as a hexafluorophosphate or as a hexafluoroantimonate salt, since these crystallize more readily than the perchlorate. Use of HCl in this reaction has been shown to give the chloromethyl complexes VIII and IX[7] instead of VII, a result consistent with the much greater nucleophilic power of Cl^-.

A two-step sequence, with second step similar to reaction 2 seems highly probable for this route to VII, involving firstly electrophilic attack by H^+ on the dimethyl complex giving the cation $[PtMe(S)(dppm)]^+$ where S = coordinated solvent.

$$[PtMe_2(dppm)] + H^+ + S \rightarrow [PtMe(S)(dppm)]^+ + CH_4 \quad (3)$$

$$[PtMe_2(dppm)] + [PtMe(S)(dppm)]^+ \rightarrow \underset{\text{VII}}{[Pt_2Me_3(\mu\text{-dppm})_2]^+} + S \quad (4)$$

Thus the second steps, (2) and (4), in the two different routes to VII both involve what may be regarded as a nucleophilic displacement, in (2) of Cl^- and in (4) of less strongly coordinated solvent molecule. It is not surprising that (4) proceeds more rapidly than (2) since the displacement of S is much easier.

Other diplatinum complexes have been obtained by somewhat similar reactions. Venanzi and his coworkers,[12] for example, have achieved the synthesis of the doubly bridged trihydrides $[Pt_2H(\mu\text{-}H)_2(PR_3)_4]^+$ (R = C_6H_5, C_2H_5, or c-C_6H_{11}) shown in reaction 5 (S = acetone). The *cis*-dihydrides

$$[PtH_2(PR_3)_2] + [PtH(S)(PR_3)_2]^+ \rightarrow [Pt_2H(\mu\text{-}H)_2(PR_3)_4]^+ + S \quad (5)$$

$[PtH_2(PR_3)_2]$ were prepared in situ in the presence of the other reagent. Ibers, Otsuka, and their coworkers[13] have proposed a similar mechanism for the formation of the singly bridged

(11) The Enraf-Nonius software package for the CAD-4F diffractometer, M. B. Hursthouse's CAD4 data processing program, a local version of G. M. Sheldrick's SHELX system, P. R. Mallinson's GEOM molecular functions program, and C. K. Johnson's ORTEP.

(12) Bracher, G.; Grove, D. M.; Venanzi, L. M.; Bachechi, F.; Mura, P.; Zambonelli, L. Proceedings of the IXth International Conference on Organometallic Chemistry, Dijon, 1979, p B26.

(13) (a) Tulip, T. H.; Yamagata, T.; Yoshida, T.; Wilson, R. D.; Ibers, J. A.; Otsuka, S. *Inorg. Chem.* **1979**, *18*, 2239. (b) Yoshida, T.; Yamagata, T.; Tulip, T. H.; Ibers, J. A.; Otsuka, S. *J. Am. Chem. Soc.* **1978**, *100*, 2063.

Table IV. Selected Interatomic Distances and Angles in $[Pt_2Me_3(\mu\text{-dppm})_2][PF_6]\cdot 3CH_2Cl_2$

Bond Lengths (Å)

Cation

Pt(1)-Pt(2)	2.769 (1)	Pt(2)-C(5)	2.06 (4)	P(2)-C(18)	1.83 (2)
Pt(1)-P(2)	2.314 (7)	P(1)-C(1)	1.83 (3)	P(2)-C(24)	1.84 (2)
Pt(1)-P(4)	2.338 (7)	P(2)-C(1)	1.82 (3)	P(3)-C(30)	1.81 (2)
Pt(1)-C(3)	2.08 (3)	P(3)-C(2)	1.85 (3)	P(3)-C(36)	1.82 (2)
Pt(1)-C(4)	2.10 (3)	P(4)-C(2)	1.87 (3)	P(4)-C(42)	1.77 (2)
Pt(2)-P(1)	2.263 (7)	P(1)-C(6)	1.83 (2)	P(4)-C(48)	1.83 (2)
Pt(2)-P(3)	2.293 (7)	P(1)-C(12)	1.82 (2)		

Anion

P(5)-F(1)	1.54 (3)	P(5)-F(3)	1.62 (4)	P(5)-F(5)	1.62 (4)
P(5)-F(2)	1.53 (3)	P(5)-F(4)	1.66 (4)	P(5)-F(6)	1.48 (5)

Solvent Molecules

C(54)-Cl(1)	1.78 (4)	C(55)-Cl(3)	1.85 (9)	C(56)-Cl(5)	1.42 (9)
C(54)-Cl(2)	1.81 (4)	C(55)-Cl(4)	1.28 (10)	C(56)-Cl(6)	2.27 (9)

Bond Angles (Deg)

Cation

Pt(2)-Pt(1)-P(2)	88.9 (2)	P(1)-Pt(2)-C(5)	87.7 (10)	Pt(2)-P(3)-C(2)	112.9 (8)
Pt(2)-Pt(1)-P(4)	84.9 (2)	P(3)-Pt(2)-C(5)	88.5 (10)	Pt(2)-P(3)-C(30)	113.8 (6)
Pt(2)-Pt(1)-C(3)	95.9 (8)	Pt(2)-P(1)-C(1)	114.8 (8)	Pt(2)-P(3)-C(36)	116.3 (7)
Pt(2)-Pt(1)-C(4)	100.0 (8)	Pt(2)-P(1)-C(6)	114.1 (7)	C(2)-P(3)-C(30)	106.6 (11)
P(2)-Pt(1)-P(4)	107.9 (2)	Pt(2)-P(1)-C(12)	113.9 (6)	C(2)-P(3)-C(36)	102.6 (11)
P(2)-Pt(1)-C(3)	83.0 (7)	C(1)-P(1)-C(6)	101.7 (12)	C(30)-P(3)-C(36)	103.4 (9)
P(2)-Pt(1)-C(4)	166.4 (8)	C(1)-P(1)-C(12)	104.8 (11)	Pt(1)-P(4)-C(2)	111.7 (9)
P(4)-Pt(1)-C(3)	169.1 (7)	C(6)-P(1)-C(12)	106.4 (9)	Pt(1)-P(4)-C(42)	112.8 (7)
P(4)-Pt(1)-C(4)	83.2 (8)	Pt(1)-P(2)-C(1)	111.5 (8)	Pt(1)-P(4)-C(48)	122.7 (7)
C(3)-Pt(1)-C(4)	85.9 (11)	Pt(1)-P(2)-C(18)	112.4 (6)	C(2)-P(4)-C(42)	102.8 (11)
Pt(1)-Pt(2)-P(1)	92.7 (2)	Pt(1)-P(2)-C(24)	121.8 (6)	C(2)-P(4)-C(48)	99.4 (11)
Pt(1)-Pt(2)-P(3)	91.1 (2)	C(1)-P(2)-C(18)	101.3 (11)	C(42)-P(4)-C(48)	105.0 (10)
Pt(1)-Pt(2)-C(5)	177.1 (10)	C(1)-P(2)-C(24)	107.2 (11)	P(1)-C(1)-P(2)	115.0 (13)
P(1)-Pt(2)-P(3)	176.2 (2)	C(18)-P(2)-C(24)	100.3 (8)	P(3)-C(2)-P(4)	111.5 (13)

Anion

F(1)-P(5)-F(2)	174.8 (18)	F(2)-P(5)-F(3)	90.5 (18)	F(3)-P(5)-F(5)	90.1 (23)
F(1)-P(5)-F(3)	92.7 (18)	F(2)-P(5)-F(4)	90.3 (17)	F(3)-P(5)-F(6)	172.3 (28)
F(1)-P(5)-F(4)	86.3 (16)	F(2)-P(5)-F(5)	90.6 (17)	F(4)-P(5)-F(5)	168.9 (19)
F(1)-P(5)-F(5)	93.5 (16)	F(2)-P(5)-F(6)	92.8 (22)	F(4)-P(5)-F(6)	94.2 (27)
F(1)-P(5)-F(6)	83.5 (21)	F(3)-P(5)-F(4)	78.8 (22)	F(5)-P(5)-F(6)	96.8 (27)

Solvent Molecules

Cl(1)-C(54)-Cl(2)	103.5 (22)	Cl(3)-C(55)-Cl(4)	121.3 (71)	Cl(5)-C(56)-Cl(6)	96.2 (49)

Torsion Angles (Deg) in the Cation

P(2)-Pt(1)-Pt(2)-P(1)	-30.7 (2)	Pt(1)-Pt(2)-P(3)-C(2)	-34.4 (9)	Pt(2)-Pt(1)-P(4)-C(42)	-163.6 (8)
C(3)-Pt(1)-Pt(2)-P(1)	52.2 (8)	Pt(1)-Pt(2)-P(3)-C(30)	87.3 (7)	Pt(2)-Pt(1)-P(4)-C(48)	69.2 (8)
P(4)-Pt(1)-Pt(2)-P(3)	41.6 (2)	Pt(1)-Pt(2)-P(3)-C(36)	-152.7 (7)	Pt(1)-P(2)-C(1)-P(1)	-35.1 (17)
C(4)-Pt(1)-Pt(2)-P(3)	-40.6 (8)	Pt(2)-Pt(1)-P(2)-C(1)	40.3 (10)	Pt(2)-P(1)-C(1)-P(2)	5.3 (18)
Pt(1)-Pt(2)-P(1)-C(1)	19.9 (10)	Pt(2)-Pt(1)-P(2)-C(18)	153.2 (7)	Pt(1)-P(4)-C(2)-P(3)	34.3 (15)
Pt(1)-Pt(2)-P(1)-C(6)	136.7 (8)	Pt(2)-Pt(1)-P(2)-C(24)	-87.9 (7)	Pt(2)-P(3)-C(2)-P(4)	6.2 (16)
Pt(1)-Pt(2)-P(1)-C(12)	-100.9 (6)	Pt(2)-Pt(1)-P(4)-C(2)	-48.4 (9)		

trihydride $[Pt_2H_2(\mu\text{-H})(L\text{-}L)_2]^+$ [L-L = $(t\text{-Bu})_2P(CH_3)_3P(t\text{-Bu})_2$] and related complexes, from the corresponding *cis*-dihydrides and chloroform according to (6) and (7). They

$$[PtH_2(L\text{-}L)] + CHCl_3 \rightarrow [PtCl(H)(L\text{-}L)] + CH_2Cl_2 \quad (6)$$

$$[PtH_2(L\text{-}L)] + [PtCl(H)(L\text{-}L)] \rightarrow [Pt_2H_2(\mu\text{-H})(L\text{-}L)_2]^+ + Cl^- \quad (7)$$

interpret reaction 7 as a nucleophilic displacement of chloride by the incoming hydrido groups of the $[PtH_2(L\text{-}L)]$ complex. In the related reactions (2) and (4) it is difficult to see which part of the $[PtMe_2(dppm)]$ molecule could act as the nucleophile, unless it is the platinum atom itself. Thus it is possible that displacement of Cl^- or S in reactions 2 and 4 occurs by attack of one platinum atom by the other and is followed by rearrangement of the dppm ligands to the bridging position. In the case of the trimethyl complex VII, because of the poor bridging ability of the methyl groups, the donor–acceptor interaction of the platinum atoms is retained as a chemical bond in the product and is revealed by the NMR and X-ray investigations described below.

Description of the Structure of $[Pt_2Me_3(\mu\text{-dppm})_2][PF_6]\cdot 3CH_2Cl_2$. The asymmetric unit of the crystal structure comprises a $[Pt_2Me_3(\mu\text{-dppm})_2]^+$ cation, PF_6^- anion, and three dichloromethane molecules. An inspection of the nonbonded interatomic contacts between different ionic molecular entities composing the structure reveals that none is shorter than the sum of the appropriate van der Waals radii by more than 0.1 Å.[14]

The atomic vibrational parameters (Tables II and III) suggest that the anions and the dichloromethane molecules are held rather loosely in the crystal structure. Indeed, it is likely that two of the CH_2Cl_2 molecules [those containing C(55) and C(56) atoms] are involved in some form of disorder. Inevitably, the geometries of these entities are rather poorly determined, as is obvious from Table IV which contains some anomalous bond lengths and angles, those involving the C(55) and C(56) atoms being particularly affected. The atoms of

(14) The hydrogen atom positions (supplementary material) used for these calculations were deduced from those of the nonhydrogen atoms, with the assumption of a C–H bond length of 1.08 Å. (The numbering of the hydrogen atoms corresponds to that of the carbon atoms to which they are bonded.) A contact radius of 1 Å has been used for hydrogen. Other van der Waals radii are taken from7: Pauling, L. "The Nature of the Chemical Bond", 3rd ed.; Cornell University Press: Ithaca, N.Y., 1960; p 260.

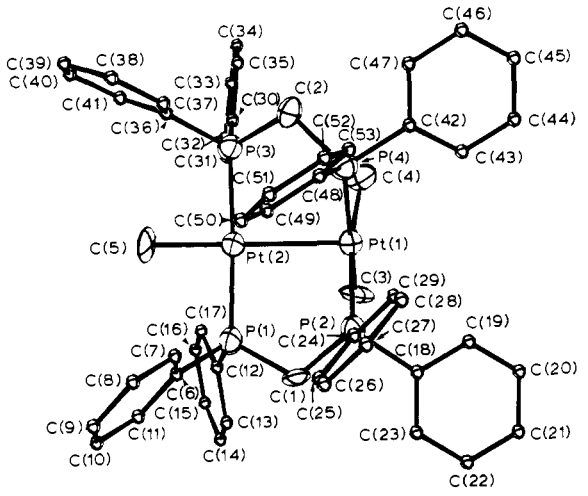

Figure 1. Perspective view of the $[Pt_2Me_3(\mu\text{-dppm})_2]^+$ cation. For clarity, hydrogen atoms are omitted and the benzene ring atoms are represented by spheres of arbitrary size. The vibrational ellipsoids of the atoms in the $Pt_2P_4C_5$ unit display 50% probability (here and in Figure 2).

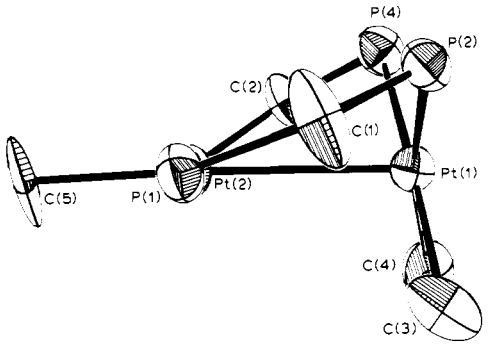

Figure 2. View of the $Pt_2P_4C_5$ unit looking down the P(1)–Pt(2)–P(3) axis.

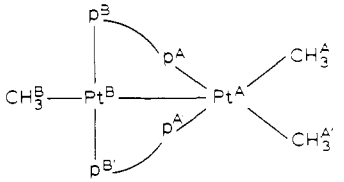

Figure 3. Labeling system used in discussing NMR results.

the cation show appreciably less thermal motion and their positions have been determined with correspondingly greater precision.

The structure of the cation (Figure 1) is of a novel type which has not been observed so far in the complexes containing an $M_2(\mu\text{-L-L})_2$ unit, where L-L = dppm and dpam (dpam = $Ph_2AsCH_2AsPh_2$). The other complexes of platinum for example which contain three ligands attached to the $M_2(L\text{-}L)_2$ unit, such as $[Pt_2Cl_2(\mu\text{-CO})(\mu\text{-dpam})_2]$,[3] adopt the A-frame geometry in which the metal centers are bridged by three ligands and are not directly bonded to one another. The inability of the methyl group to function as a bridging ligand evidently precludes such a structure for the $[Pt_2Me_3(\mu\text{-dppm})_2]^+$ cation. Instead, the platinum atoms are directly bonded to one another, as well as being bridged by both dppm ligands. Two of the methyl groups are attached to Pt(1) and the third is attached to Pt(2).

Nearly exact square-planar coordination is found around Pt(2). The Pt(2)–P bonds are mutually trans [P(1)–Pt(2)–P(3) = 176.2 (2)°], as are the Pt(2)–C(5) and Pt(2)–Pt(1) bonds [Pt(1)–Pt(2)–C(5) = 177 (1)°]. The angles subtended by cis ligand donor atoms at Pt(2) are all within 3° of 90°, and the deviations of the atoms Pt(1), Pt(2), P(1), P(3), and C(5) from their common plane do not exceed 0.04 Å. An unusual type of fivefold coordination is found around Pt(1). Two cis methyl carbon atoms C(3) and C(4) and two cis phosphorus atoms, P(2) and P(4), belonging to different dppm ligands, define a rather irregular square plane about Pt(1). The cis P(2)–Pt(1)–P(4) angle of 107.9 (2)° deviates appreciably from 90°, and a significant tetrahedral distortion is indicated by the displacement of atoms from the $Pt(1)P_2C_2$ mean plane [Pt(1) −0.056, P(2) 0.082, P(4) −0.051, C(3) −0.075, C(4) 0.10 Å]. The Pt(1)–Pt(2) bond vector is tilted by 9° away from the normal to this mean plane and toward the phosphorus atoms, so that the Pt(2)–Pt(1)–P angles are 84.9 (2) and 88.9 (2)°, whereas the Pt(2)–Pt(1)–C angles are 95.9 (8) and 100.0 (8)° (see Figure 2).

The Pt–P and Pt–C distances in the cation are in accord with corresponding values in square-planar platinum(II) complexes. Thus the Pt(1)–P bond lengths of 2.314 (7) and 2.338 (7) Å may be compared with values of 2.310 (7) and 2.326 (1) Å for Pt^{II}–P (trans to σ-C) bonds in *cis*-$[PtF\{CH(CF_3)_2\}(PPh_3)_2]$[15] and *cis*-$[Pt(CF_3)_2(PMe_2C_6F_5)_2]$.[16] The Pt(2)–P distances of 2.263 (7) and 2.293 (7) Å lie within the range of 2.25–2.33 Å found for Pt^{II}–P (trans to P) bonds involving phosphines with phenyl or *n*-alkyl substituents.[17] Their shortness, relative to the Pt(1)–P distances, may reflect the different coordination numbers of the two platinum atoms as well as the differing trans influence they experience. Pt(II)–C(alkyl) bond lengths show a large range, from 2.01 (1) to 2.18 (1) Å.[18,19] All the values found here lie near the center of this range and agree particularly well with the Pt–C (trans to P) bond length of 2.07 (2) Å in *cis*-$[PtF\{CH(CF_3)_2\}(PPh_3)_2]$.[15]

Both Pt_2P_2C rings have rather similar envelope conformations (Figure 2) with Pt(2)–P(1)–C(1)–P(2) and Pt(2)–P(3)–C(2)–P(4) torsion angles, respectively 5 (2) and 6 (2)°, not significantly different from zero (Figure 2). As a result, the cation, excluding the peripheral phenyl groups, has approximate *m* symmetry, the mirror plane being perpendicular to the coordination plane of Pt(2) and bisecting the P–Pt(1)–P and C–Pt(1)–C angles. The P(2)–Pt(1)–Pt(2)–P(1) and P(4)–Pt(1)–Pt(2)–P(3) torsion angles of −30.7 (2) and 41.6 (2)° appear to be determined mainly by the bite of the dppm ligands [P(1)···P(2) = 3.077, P(3)···P(4) = 3.080 Å], which is considerably greater than the length of the Pt–Pt bond bridged by these ligands. Values of ±45° for these torsion angles are required if repulsions between filled nonbonding d orbitals of the different metal atoms are to be minimal.

The number of short interligand and Pt···H nonbonded contacts[14] within the cation suggests that overcrowding is severe.[20-23] Bond lengths and angles within the dppm ligands are unexceptional. The dihedral angles between the planes of geminal phenyl rings show no obvious pattern. They vary from 64 to 86°, the individual values being presumably determined by packing requirements.

(15) Howard, J.; Woodward, P. *J. Chem. Soc., Dalton Trans.* **1973**, 1840.
(16) Manojlović-Muir, Lj.; Muir, K. W.; Solomun, T.; Meek, D. W.; Peterson, J. L. *J. Organomet. Chem.* **1978**, *146*, C26.
(17) Muir, K. W. *Spec. Period. Rep.: Mol. Struct. Diffr. Methods* **1973**, *1*, 606; **1975**, *3*, 371; **1976**, *4*, 307.
(18) Robertson, G. B.; Whimp, P. O. *Inorg. Chem.* **1974**, *13*, 2082.
(19) Rush, P. E.; Oliver, J. D. *J. Chem. Soc., Chem. Commun.* **1974**, 996.
(20) La Placa, S. J.; Ibers, J. A. *Inorg. Chem.* **1965**, *4*, 778.
(21) Matsumoto, M.; Yoshioka, H.; Nakatsu, K.; Yoshida, T.; Otsuka, S. *J. Am. Chem. Soc.* **1974**, *96*, 3322.
(22) Immirzi, A.; Musco, A. *J. Chem. Soc., Chem. Commun.* **1974**, 400.
(23) Hitchcock, P. B.; Lappert, M. F.; Pye, P. L. *J. Chem. Soc., Chem. Commun.* **1977**, 196.

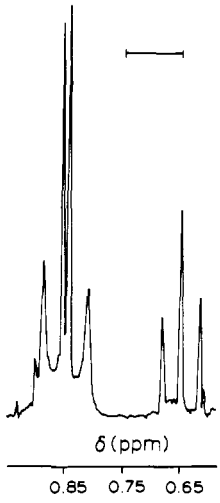

Figure 4. $^1H\{^{195}Pt\}$ NMR spectrum (200 MHz) of $[Pt_2Me_3(\mu\text{-dppm})_2][PF_6]$ showing only the methylplatinum region. The bar represents 20 Hz.

Analysis of ^1H and ^{31}P NMR Spectra. The chief structural features of the complex were initially deduced from an analysis of the ^1H NMR spectrum (in the region of the methylplatinum resonances) and of the $^{31}P\{^1H\}$ NMR spectrum.[5] The labeling system for the atoms is defined in Figure 3, and a diagram of the $^1H\{^{195}Pt\}$ NMR spectrum (200 MHz) in the methylplatinum region is shown in Figure 4. There are two resonances in this region, and these are discussed briefly below.

1. A methylplatinum resonance at δ 0.85 of relative intensity 2 is due to the methyl groups on Pt^A and shows the second-order splittings due to coupling with ^{31}P usually observed for molecules with the *cis*-$[PtMe_2P_2]$ grouping.[24] The peaks of the sharp closely spaced doublet (Figure 4) are separated by $^3J(H^AP^A) + {}^3J(H^AP^{A'}) = 2.3$ Hz. Selective ^{31}P decoupling experiments proved that this coupling was due to P^A and $P^{A'}$. In the ^{195}Pt-coupled spectrum, satellites of one-fourth intensity with $^2J(Pt^AH^A) = 60$ Hz were observed, and longer range coupling with Pt^B was also indicated with $J(Pt^BH^A) = 6$ Hz. This latter coupling was just resolved in the ^{31}P-decoupled spectrum.[5]

2. A methylplatinum resonance at δ 0.65 of relative intensity 1 is due to the methyl group on Pt^B and appears as a 1:2:1 triplet due to coupling with P^B and $P^{B'}$ with $^3J(P^BH) = 6.5$ Hz. In the ^{31}P-decoupled spectrum, satellites due to coupling with both Pt^B and Pt^A were clearly observed with $^2J(Pt^BH^B) = 80.5$ Hz and $J(Pt^AH^B) = 11$ Hz.[5]

The resonance due to the CH_2P_2 groups of the ligand occurs at δ 3.86. The resonance appears as a complex unresolved multiplet and has not been analyzed in detail.

The $^{31}P\{^1H\}$ NMR spectrum of the complex is shown in Figure 5. The spectrum has superimposed resonances due to isotopomers containing no ^{195}Pt atoms (43.8%), one ^{195}Pt atom (44.8%) with an equal probability of being Pt^A or Pt^B, and two ^{195}Pt atoms (11.4%). The majority of the intense peaks in the central part of the spectrum arise from molecules containing no ^{195}Pt atom, and the atoms $P^AP^{A'}P^BP^{B'}$ form an [AA'BB'] coupling system, which is difficult to interpret from first principles. Fortunately, the spectra due to molecules containing one ^{195}Pt atom are easier to interpret. Thus, if for example Pt^A is the ^{195}Pt atom, satellites are formed centered about $\delta(P^A)$ with separation of $^1J(Pt^AP^A)$ and about $\delta(P^B)$ with separation $^2J(Pt^AP^B)$. The outer satellites due to $^1J(Pt^AP^A)$

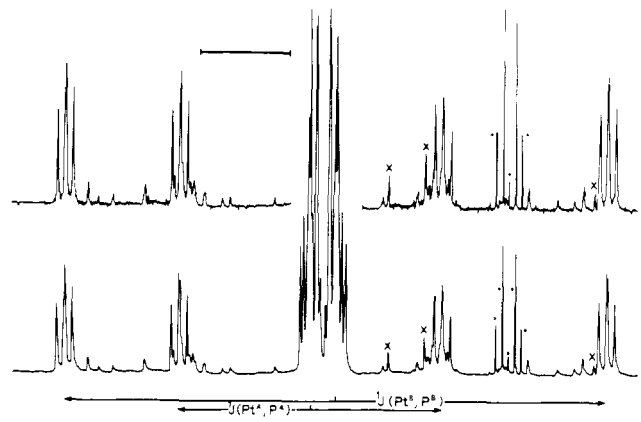

Figure 5. $^{31}P\{^1H\}$ NMR spectrum (40.5 MHz) of $[Pt_2Me_3(\mu\text{-dppm})_2][PF_6]$, showing $\delta(P^A)$, $\delta(P^B)$, $^1J(Pt^AP^A)$, and $^1J(Pt^BP^B)$. Peaks marked * are due to reference $(MeO)_3PO$ and those marked × are due to impurities. The bar represents 500 Hz.

are easily identified, thus defining $\delta(P^A)$ 27.13 and $^1J(Pt^AP^A) = 1459$ Hz. The low value of $^1J(Pt^AP^A)$, similar to that found in monomeric $[PtMe_2(dppm)]$[7,8] confirms the assignment of P^A trans to methyl. In addition, the satellites show splittings due to coupling with P^B and $P^{B'}$ and the couplings $J(P^AP^B)$ and $J(P^AP^{B'})$ can be measured directly as 45 and 42 Hz, though the specific assignments cannot be made. Similarly, when Pt^B is the ^{195}Pt atom, satellites are centered about $\delta(P^B)$ 23.66 with separation of $^1J(Pt^BP^B) = 3009$ Hz. Now, knowing the chemical shifts and some of the coupling constants, it was possible to simulate the central [AA'BB'] spectrum by using the computer program LAOCN3. The magnitude of $J(P^AP^B)$ was thus confirmed as 45 Hz, and the long-range couplings $J(Pt^AP^B)$ and $J(Pt^BP^A)$ (both ~15 Hz) were identified. Reasonable values from the literature of $^2J(P^AP^{A'}) = 50$ and $^2J(P^BP^{B'}) = 500$ Hz were assumed in the simulations,[25] but the spectra were, as expected, rather insensitive to changes in these couplings and they could not be refined.

Finally the molecules containing two ^{195}Pt atoms give rise to an [AA'BB'MX] spin system, and many of the weak lines in the ^{31}P spectrum could be assigned to this spin system. Computer simulation using coupling constants derived from the above analysis and varying the extra coupling constant $^1J(MX) = {}^1J(Pt^APt^B)$ allowed this coupling constant to be determined as 332 Hz. Thus a rather complete analysis of this complex spectrum was accomplished. The spectrum is clearly fully consistent with the solid-state structure determined by X-ray studies and it is clear that the molecule is not fluxional on the NMR time scale.

Bonding in the Complex. The details of the coordination geometries around Pt(1) and Pt(2) suggest that the bonding between these atoms involves donation of electron density from the filled d_{z^2} orbital of the square-planar $[Pt(1)P_2C_2]$ species into a vacant acceptor orbital of the $[Pt(2)P_2C]^+$ unit. Both metal atoms are then in a formal oxidation state of +2, and they each attain a 16-electron count; the bonding is represented in A below. An alternative description (B) considers the complex as containing a homopolar Pt(I)–Pt(III) covalent bond, but this differs from A only in the extent of sharing of the electron pair in the Pt–Pt bond. The relatively long Pt–Pt bond of 2.769 (1) Å is consistent with the weaker interaction expected for A. Thus in a recent survey of Pt–Pt distances it has been pointed out that the majority of such bonds are substantially shorter than 2.77 Å although the complete range is 2.60–3.00 Å.[13] The heteropolar metal–metal bond formulated in A is not without precedent; the isoelectronic Ir(I) is

(24) (a) Greaves, E. O.; Bruce, R.; Maitlis, P. M. *J. Chem. Soc., Chem. Commun.* **1967**, 860. (b) Ruddick, J. D.; Shaw, B. L. *J. Chem. Soc. A* **1969**, 2801. (c) Goodfellow, R. J.; Hardy, M. J.; Taylor, B. F. *J. Chem. Soc., Dalton Trans.* **1973**, 2450.

(25) Pregosin, P. S.; Kunz, R. W. "^{31}P and ^{13}C NMR of Transition Metal Phosphine Complexes"; Springer-Verlag: Berlin, 1979.

considered to form such a bond to BF_3 in the adduct $[IrCl(CO)(PPh_3)_2(BF_3)]$.[26]

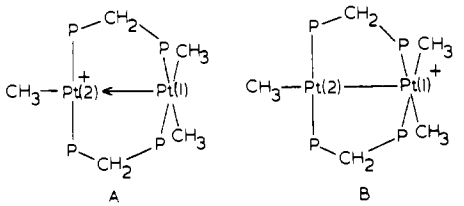

A B

According to formalism B, however, the Pt(1) atom is considered to participate in the formation of a homopolar Pt–Pt bond and to exhibit an oxidation state of +3. As such it might therefore be expected to be electronically similar to Pt(IV) and to have the usual octahedral coordination and 18-electron count typical of this oxidation state. This is in fact the case in the structurally characterized diplatinum(III) complexes $[Pt_2Me_4(\mu\text{-}CF_3CO_2)_2(4\text{-Me-py})_2]$[27] and $[Pt_2(\mu\text{-}SO_4)_4(H_2O)_2]^{2-}$.[28] In these complexes, each platinum atom achieves octahedral coordination by binding a ligand in the position trans to the Pt–Pt bond. In contrast, however, this position in complex VII is vacant. Moreover, this complex does not coordinate an additional ligand when treated with ammonia or pyridine (although it is decomposed by organophosphines). This suggests considerable residual electron density in the d_{z^2} orbital, and therefore incomplete sharing of the electron pair in the Pt–Pt bond and thus an oxidation state of +2 rather than +3.

Further information can be obtained by consideration of the magnitudes of coupling constants involving ^{195}Pt. It has been shown that in binuclear platinum(I) complexes of general formula $[Pt_2XY(\mu\text{-dppm})_2]$ containing a covalent Pt–Pt bond, the Pt–Pt bond exerts a high trans influence comparable to that of a tertiary phosphine ligand. This can be seen from the magnitudes of $^1J(PtX)$ or $^1J(PtY)$ (e.g., X, Y = H or PR_3) trans to the Pt–Pt bond[29,30] and from bond distances trans to the Pt–Pt bond.[29,31] However, the coupling constant $^2J[(Pt(2)CH_3]$ in complex VII is 80.5 Hz, indicating that in this complex the Pt–Pt bond exerts a low trans influence.[32] The trans influence is closer to that of Cl^- in $[Pt_2Me_2(\mu\text{-Cl})(\mu\text{-dppm})_2]^+$, $^2J(PtCH_3)$ = 88 Hz,[7] than to that of tertiary phosphine in $[Pt_2Me_4(\mu\text{-dppm})_2]$, with $^2J(PtCH_3)$ = 70 Hz.[33] The result indicates that the orbital of Pt(2) involved in the Pt–Pt bond has rather little s character, and this is, of course, consistent with the long Pt–Pt distance established by the X-ray structure and with the low value of $^1J(Pt\text{–}Pt)$.[30]

That there is some s character contribution from Pt(1), however, is indicated by consideration of the coupling constants about this platinum atom. The closest structural analogy is in the cis dimer $[Pt_2Me_4(\mu\text{-dppm})_2]$, in which there is no evidence for Pt–Pt interaction and for which $^2J(PtMe)$ = 70 Hz and $^1J(PtP)$ = 1830 Hz.[33] The lower values found for VII, of 60 and 1459 Hz, respectively, are indicative of lower s character within the $Pt(1)C_2P_2$ plane and hence are evidence of some s character having been transferred to the Pt–Pt bond.

Thus within the constraints of the oxidation state formalism, the bonding seems best described as a Pt(II)→Pt(II) donor–acceptor interaction and represents an unusual example of heteropolar metal–metal bonding. This class of bonding was first invoked by Hock and Mills[34] in their description of the structure of the binuclear complex $[Fe_2(CO)_6\{C_4Me_2(OH)_2\}]$ (IX) and has since been postulated by Lewis and coworkers[35] to account for the bonding and reactivity of the hexanuclear cluster $[Os_6(CO)_{18}]$ (X).

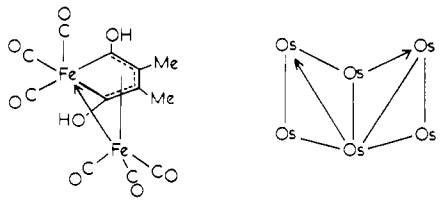

IX X

Finally, comparison of complex VII with the dirhodium complex $[Rh(CO)RhCl_2\{\mu\text{-}(PhO)_2PN(Et)P(OPh)_2\}_2]$,[4] the only other known structurally analogous complex, may be made. In contrast to our proposals for VII, Haines et al. describe the structure in terms of a mixed-valence Rh(0)/Rh(II) complex containing a homopolar Rh–Rh bond although an alternative description as a birhodium(I) complex containing a Rh(I)→Rh(I) donor–acceptor bond is a possibility.

Acknowledgment. We thank the NSERC (Canada) for financial support (to R.J.P.), NATO for a travel grant (to M.P.B. and R.J.P.), and the SRC for the award of an Advanced Fellowship (to K.R.S.) and a Research Studentship (to S.J.C.). We also thank Dr. D. J. Cole-Hamilton for helpful discussions and Dr. W. E. Hull of Bruker Analytische Mestechnik GmbH for ^1H NMR spectra (WP-200).

Registry No. VIIa·$3CH_2Cl_2$, 76584-40-2; VIIb, 76600-28-7; VIIc, 73464-61-6; VIII, 76584-41-3; $PtMe_2$(dppm), 52595-90-1; $PtCl_2$(dppm), 52595-94-5; HPF_6, 16940-81-1; $HSbF_6$, 16950-06-4; $HClO_4$, 7601-90-3.

Supplementary Material Available: Listings of observed and calculated structure factors and H atom fractional coordinates (33 pages). Ordering information is given on any current masthead page.

(26) Scott, R. N.; Shriver, D. F.; Lehman, D. D. *Inorg. Chim. Acta* **1970**, *4*, 73.
(27) Schagen, J. D.; Overbeek, A. R.; Schenk, H. *Inorg. Chem.*, **1978**, *17*, 1938.
(28) Muraveiskaya, G. S.; Kukina, G. A.; Orlova, V. S.; Evstaf'eva, O. N.; Porai-Koshits, M. A. *Dokl. Chem. (Engl. Transl.)* **1976**, *226*, 76.
(29) Brown, M. P.; Fisher, J. R.; Manojlović-Muir, Lj.; Muir, K. W.; Puddephatt, R. J.; Thomson, M. A.; Seddon, K. R. *J. Chem. Soc., Chem. Commun.* **1979**, 931, and unpublished results.
(30) Brown, M. P.; Franklin, S. J.; Puddephatt, R. J.; Thomson, M. A.; Seddon, K. R. *J. Organomet. Chem.* **1979**, *178*, 281.
(31) (a) Brown, M. P.; Puddephatt, R. J.; Manojlović-Muir, Lj.; Muir, K. W.; Solomun, T.; Seddon, K. R. *Inorg. Chim. Acta* **1977**, *23*, L33. (b) Manojlović-Muir, Lj.; Muir, K. W.; Solomun, T. *Acta Crystallogr., Sect B* **1979**, *B35*, 1237.
(32) Appleton, T. G.; Clark, H. C.; Manzer, L. E. *Coord. Chem. Rev.* **1973**, *10*, 335.
(33) Brown, M. P.; Puddephatt, R. J.; Thomson, M. A., unpublished work.
(34) Hock, A. A.; Mills, O. S. *Acta Crystallogr.* **1961**, *14*, 139.
(35) John, G. R.; Johnson, B. F. G.; Lewis, J. *J. Organomet. Chem.* **1979**, *181*, 143.